Validating Nominal Bias Error Limits Using 4 years of WAAS Signal Quality Monitoring Data

R. Eric Phelts, *Stanford University*
Eric Altshuler, *Sequoia Research Company*
Todd Walter, Per Enge, *Stanford University*

BIOGRAPHY

R. Eric Phelts, Ph.D., is a research engineer in the Department of Aeronautics and Astronautics at Stanford University. He received his B.S. in Mechanical Engineering from Georgia Institute of Technology in 1995, and his M.S. and Ph.D. in Mechanical Engineering from Stanford University in 1997 and 2001, respectively. His research involves signal deformation monitoring techniques and analysis for SBAS and GBAS.

Dr. Eric Altshuler received his B. S. in mathematics and computer science from UCLA in 1989 and his Ph.D. in physics in 1998 from University of California at Irvine. He is currently a Senior Software Engineer at Sequoia Research Company and is active in the development and implementation of ionospheric algorithms and prototyping for WAAS.

Todd Walter, Ph.D., is a senior research engineer in the Department of Aeronautics and Astronautics at Stanford University. Dr. Walter received his Ph.D. from Stanford and is currently working on modernization of the Wide Area Augmentation System (WAAS) and defining future architectures to provide aircraft guidance. Key contributions include early prototype development proving the feasibility of WAAS, significant contribution to the WAAS MOPS, design of ionospheric algorithms for WAAS, and development of dual frequency algorithms for SBAS. He is a fellow of the Institute of Navigation and serves as its president.

Per Enge, Ph.D., is a professor of aeronautics and astronautics at Stanford University, where he is the Kleiner-Perkins Professor in the School of Engineering. He directs the GNSS Research Laboratory, which develops satellite navigation systems. He has been involved in the development of the Federal Aviation Administration's GPS Wide Area Augmentation System (WAAS) and Local Area Augmentation System (LAAS). For this work, Enge has received the Kepler, Thurlow, and Burka awards from the Institute of Navigation (ION). He received his Ph.D. from the University of Illinois. He is a member of the National Academy of Engineering and a Fellow of the IEEE and the ION

ABSTRACT

Nominal signal deformations are small imperfections of GNSS signals that cause them to differ from one another. While generally small, they exist on all SV signals and potentially lead to user range biases that are present all the time. These subtle effects have been measured in the past using specialized equipment and processing techniques and also using more conventional receivers as well.

Augmentation systems such as SBAS, GBAS and ARAIM rely on assumptions about the magnitudes and the stability of these biases to ensure safe, high-integrity navigation for aviation users at all times. However, little is known about how these distortions evolve over time, how they are affected by satellite configuration and system changes, or how well the existing continuously-operating, signal monitors can measure these nominal biases.

To this end, this paper analyzes approximately 4.5 years of continuous WAAS signal deformation monitoring (SDM) measurements that have been collected. The results are used to assess the evolution of nominal signal distortions of the L1 C/A coed signals from all the GPS satellites in operation over this time period. Old and new satellites are compared and changes due to potential anomalies or system changes are discussed. It is shown that the WAAS signal deformation monitor measurements agree with past high-resolution measurements of nominal signal deformations, and that they are very sensitive to changes in the signal deformations. And, while the signals are quite stable and significant signal deformation

events tend to be rare, unexpected changes can occur. Accordingly, the maximum nominal range biases on the C/A codes of the current GPS constellation may be quite close to the range error limit required to guarantee integrity of future dual-frequency WAAS aviation users.

WAAS SIGNAL DEFORMATION MONITORING

The Wide Area Augmentation System (WAAS) has performed integrity monitoring of the GPS constellation since 2003. The WAAS ground reference receiver network consists of 138 continuously operating reference receivers—3 at each of 46 reference stations located in the U.S. Canada and Mexico—capable of measuring the quality of the GPS signals on L1 in several ways. In particular, these receivers are equipped with multiple correlators on each channel which are used to measure relative distortions of the C/A codes of all the satellites in view.

The current reference receivers each have an 18MHz front-end bandwidth and use early-minus-late tracking at 0.1-chip spacing on L1 (C/A). Each signal channel has a total of 8 correlator outputs (not including Prompt), located at the following offsets (as measured in fractions of a C/A code chip): [-0.1023 -0.076 -0.05115 0.025 Prompt 0.025 0.05115 0.076 0.1023].

The WAAS signal deformation monitor (SDM) uses these nine correlator measurements to measure the amount of correlation peak distortion a given signal experiences, relative to the others. To accomplish this with multiple conventional receivers and antenna hardware, the monitor must cope with noisy measurements including biases from multipath, receivers, and even the ideal PRN codes peaks themselves. If not properly accounted for, these can partially obscure hazardous, anomalous signal faults from detection and also potentially alter its estimates of nominal signal distortions. To properly assess the trends in the latter over time, the process taken to form the real-time detection metrics (which attempt to account for the measurement biases) must be carefully considered.

Processing for WAAS SDM includes the following six primary steps:

1. Normalization (Amplitude Variation Removal)
2. Time-Smoothing and Metric Computation (Thermal and Environmental Noise Removal)
3. Multiple Receiver Averaging (Receiver Bias and Multipath Removal)
4. PRN Code Normalization (Correlation Peak Type Bias Removal)
5. Reference Bias Computation (Median Distortion Removal)
6. Threshold Comparison (Fault Detection)

Each of these steps is described below.

1. Normalization (Amplitude Variation Removal)

The magnitude of the correlation peak can vary significantly due to signal power variations and multipath. Amplitude normalization is needed to reduce these effects on the measurements.

For every satellite *i* observed by receiver *j*, each of the 8 correlator measurements (located at a code offset *x*) are first normalized by the prompt *P* measurement according to

$$\left[R(x)\right]_i^j = \frac{\left[I_x\right]_i^j}{\left[I_0\right]_i^j} = \frac{\left[I_x\right]_i^j}{\left[P\right]_i^j} \tag{1}$$

2. Time-Smoothing and Metric Computation (Thermal and Environmental Noise Removal)

The raw correlator measurements R_x are filtered using a first order filter of time constant *F* (50 seconds). The normalized, filtered measurements R'_x at each time step *t* are given by

$$\left\{\left[R'_x\right]_j^i(t)\right\} = \frac{1}{F}\left\{\left[R_x\right]_j^i(t)\right\} + \frac{F-1}{F}\left\{\left[R'_x\right]_j^i(t_{prev})\right\} \tag{2}$$

The detection metrics used to measure the signal distortion on the codes are comprised of linear combinations of the 8 correlator outputs tuned to the correlation peak shape and correlator configuration of the WAAS reference receivers. Given the receiver (i.e., filter and correlator) configuration and the signal deformation threat model, each metric proposes to maximize the ratio of the mean metric value to its expected standard deviation [1].

The expression for the *m*th metric *D*(*t*) is

$${}^{m}D_j^i(t) = \left[\overline{\Gamma}^{\mathrm{T}}\right]_j^i {}^{m}\overline{\alpha} \tag{3}$$

where $\overline{\Gamma}$ is a column vector of filtered correlator outputs and is the ${}^{m}\overline{\alpha}$ is the *m*th detection metric column vector of weights α_x, each at code offset *x*. WAAS currently uses a total of 4 metrics (i.e., *m* = 1 to 4).

3. Multiple Receiver Averaging (Receiver Bias and Multipath Removal)

To further reduce the effects of noise and multipath, metrics from many receivers are averaged together. However, manufacturing tolerances and temperature variations from receiver-to-receiver can cause the same metrics (on the same SV signal) from two or more receivers to differ significantly. It can also cause the measurements to slowly drift independently over time. For these reasons, prior to averaging across receivers, the inter-receiver biases (IRBs) must be estimated and removed.

To estimate the IRBs, highly-smoothed moving averages of the metrics are taken. These are then averaged across all received signals for each receiver. This IRB ${}^{m}\hat{b}_j^i(t)$ is then subtracted from the corresponding metrics from all SVs in that receiver. (More details of this procedure are provided in the Appendix.) The weighted average of all (*J*) receivers is then given by:

$$ {}^{m}\hat{D}^i(t) = \sum_{j=1}^{m J^i} {}_{m}w_j^i(t)\left[{}^{m}D_j^i(t) - {}^{m}\hat{b}_j^i(t)\right] \qquad (4) $$

where ${}_{m}w_j^i(t)$ are the metric weights, which are defined by *a priori* functions of the metric standard deviations. (Refer to the Appendix.)

4. PRN Code Normalization (Correlation Peak Type Bias Removal)

The ideal autocorrelation of GPS C/A PRN codes produce autocorrelation peaks codes that have fairly significant side lobes. When these side lobes occur flush against the main peak, its shape (i.e., slope) may be slightly altered—either slightly narrower or wider than normal [2]. Once analyzed together with the receiver filter characterization (and the aforementioned steps), these deterministic differences can be computed offline then simply subtracted off. Equation 5 below shows this operation and represents the type bias for SV *i* as B_ζ, where ζ is the PRN code type; it ranges from 1 to 3.

$$ {}^{m}\overline{D}^i(t) = {}^{m}\hat{D}^i(t) - {}^{m}B_\zeta \qquad (5) $$

Without this step, the metrics for specific PRNs with "skinny" correlation peaks would always be slightly offset relative to those with "fat" peaks. And it follows that these two types would produce metrics offset relative to other PRNs (the majority of which produce correlation peaks with moderate or "normal" slopes). Any of these large offsets would make subsequent SV-to-SV deformation comparisons (i.e., Step 6) impossible.

5. Reference Bias Computation (Median Distortion Removal)

Ideal (infinite bandwidth, zero-distortion) signals that have no signal distortion in an absolute sense are unrealizable. Real-world hardware (e.g., bandlimited, manufactured components) always introduces some small amounts of signal distortion. However the more closely-matched the received signals are, the smaller the resulting use range error. This implies that the best signal is the one that most resembles all the others.

The signal deformation monitor defines the "best" metric (and, by extension, the "best" C/A code signal) as the median across all those visible by WAAS at any given time. This effectively asserts that the metrics of any ranging signal that differs from this will result in a range error. The median-adjusted metric ${}_{m,adj}\overline{D}^i(t)$ is thus given by Equation (6).

$$ {}_{m,adj}\overline{D}^i(t) = {}^{m}\overline{D}^i(t) - \underset{i}{median}\left[{}^{m}\overline{D}^i(t)\right] \qquad (6) $$

This (final) detection metric accommodates the fact that nominal monitor (and range error) biases will be ever-present and non-zero [3]. In addition, it effectively creates a detector that is sensitive to more than just anomalies as defined by the specific threat model the metrics were designed to mitigate [1]. This implementation further anticipates the fact that signal deformations (of any form) that differ substantially from the norm are the ones that are the most potentially hazardous to aviation users.

6. Threshold Comparison (Fault Detection)

The detection test for each SV is simply ${}_{m,adj}\overline{D}^i(t)$ divided by the threshold ${}_{m}T^i$ (and maximized over all metrics *m*). The threshold is determined from the total number of receivers *J* viewing each SV and the elevation angles θ_j^i to each of them. Equation (7) provides this expression.

$$ {}_{m}T^i = K_{ffd} \cdot \sum_{j=1}^{J} {}_{m}\sigma_j^i\left(\theta_j^i\right) = K_{ffd}\ {}_{m}\sigma^i \qquad (7) $$

In the above equation, K_{ffd} is the constant found from the fault-free probability of false alarm, and ${}_{m}\sigma_j^i\left(\theta_j^i\right)$ is the *a priori* sigma as a functon of elevation angle and metric *m*.

The final detection test for the SDM is then

$$\bar{D}^i_{\max}(t) = \max_m \left(\frac{{}_{m,adj}\bar{D}^i(t)}{{}_mT^i} \right) \quad (8)$$

where

$$\bar{D}^i_{\max}(t) \begin{cases} \geq 1, & \textit{Anomalous deformation detected} \\ < 1, & \textit{Nominal operation} \end{cases} \quad (9)$$

Ideally, $\bar{D}^i_{\max}(t)$ would have a nominal mean that is nearly zero at all times. This would indicate that all the SV signals were nearly identical to each other. However, due to the presence of nominal signal deformations, this metric has small SV-dependent biases [3]. The statistics and trends of Equation (8) can reveal how GPS SV nominal signal deformation (and, consequently, user range error) biases have evolved over time.

ANALYSIS

High-resolution Signal Captures (Dish Data)

Most prior work with nominal signal deformation analyses leverage signal data captured with the aid of high-gain, parabolic "dish" antennas [4][5][6][7][8]. These provide superior signal-to-noise ratios and very low-multipath signals. They also yield high-resolution captures of the signals [9]. (See Figures 1 and 2.) These high-resolution signal captures can subsequently be used to analyze the signals in a number of ways, including analysis of the monitor metric $\bar{D}^i_{\max}$ and receiver error modeling.

This kind of "dish data" has several limitations, however [10]. For one, it requires specialized hardware (e.g., large directional antennas, high-fidelity signal analyzers) to obtain. In addition, because the antennas are highly-directional, they can only view a single SV at a time. Finally, these are generally brief, snapshots of the signals taken only at an instant in time. Seconds are usually all that are required; continuous, long-term dish data spanning days, months or years is generally unavailable. Real-time processing is also impractical for monitoring purposes. For this reason, WAAS signal quality monitors, using its real-time network of SDM (multi-correlator) receivers and multiple years of collected data, compliments past and present nominal bias analyses.

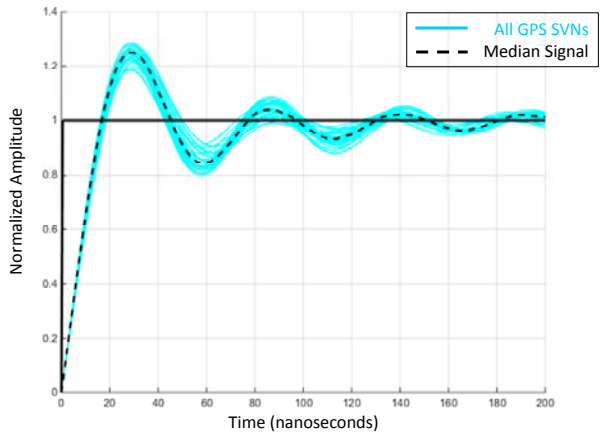

Figure 1. High-resolution "Dish Data" C/A code transitions. (Median reference signal also shown.) Dish Data collected on August 1, 2010.

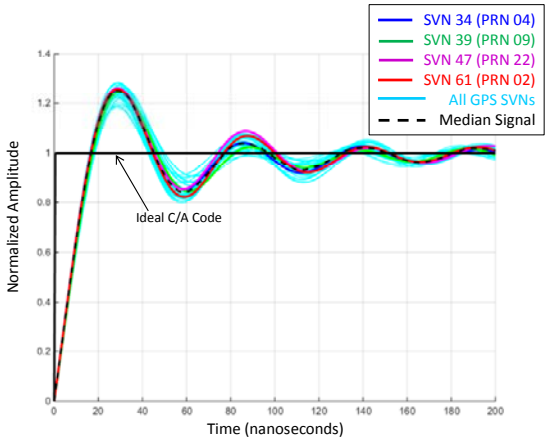

Figure 2. High-resolution "Dish Data" C/A code transitions. Signals from SVNs 34 (04), 39 (PRN 09), 47 (PRN 22), and 61 (PRN 02) are highlighted. (Median reference signal also shown.) Data collected on August 1, 2010.

Equations (1) though (8) can be used to compute the WAAS metric values corresponding to the high-resolution dish data. Figure 3 plots the corresponding $\bar{D}^i_{\max}$ for the nominally deformed SV signals of Figure 2. The SVNs are plotted in launch order and they are separated by block type as in [9]. Note that four SVNs have been highlighted in both of these figures for illustration purposes. They are SVNs 34 (04), 39 (PRN 09), 47 (PRN 22), and 61 (PRN 02). These four SVNs will be discussed later to provide further insights into the WAAS SDM data and nominal bias trends.

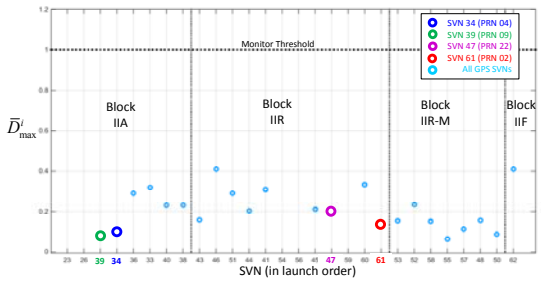

Figure 3. WAAS SDM metrics $\bar{D}^i_{\max}$ computed from high-resolution "dish data". (Dish Data collected on August 1, 2010.)

User Range Error vs. WAAS SDM Metric

User range errors can also be estimated from the dish data by simply applying the receiver filter and correlator/discriminator models to the captured code sequences. Current WAAS user receivers have correlator spacings, filter bandwidths and group delays constrained as specified in the WAAS Minimum Operational Performance Standard DO-229D [11].

These constraints are relatively loose for current (single-frequency, L1-only) WAAS users. For instance, they span a wide array of correlator spacings—from 0.05 to 1.0-chip (for early-minus-late discriminators). Filter bandwidths for these users range from 2 MHz to 20 MHz. For future, dual-frequency WAAS receivers, however, it has been proposed that the range of user correlator spacings be limited to between 0.08 and 0.12 chips on C/A code. And pre-correlation filter bandwidths would be constrained to between 12 MHz and 24 MHz. [12]

These constraints reduce the expected nominal bias error by limiting designs to those more closely aligned with the future WAAS reference receiver configuration—24 MHz and 0.1-chip (early-minus-late) on C/A code. The user receiver configurations for L5 will also be similarly constrained; however, L5 code nominal biases and errors are beyond the scope of this paper.

Using the measured waveforms of Figure 2, the aforementioned avionics receiver constraints can be used to model the corresponding worst-case user range error for each of these SVs as well. The maximum user range error bound can then be computed as a function of signal deformation metric $\bar{D}^i_{\max}$. The result is plotted in Figure 4. Observe that, the metric-dependent range error bound—the multi-level curve that overbounds the data—is assumed to monotonically increase as a function with monitor metric. In other words, range error bound for any given metric value can never be smaller than the bound corresponding to a smaller metric value.

Figure 4 also shows the nominal bias limit for current (single-frequency) WAAS users and a much smaller one for for future (dual-frequency) WAAS users. Between these two, is a proposed 27 cm limit for ARAIM users. (This ARAIM bias limit on L1 C/A code assumes a total dual-frequency nominal bias error of 75 cm [12], and allows for up to 11 cm of nominal bias on L5 [13]. Then, accounting for the scale-factors to remove of the ionosphere— 2.26 on L1 and 1.26 on L5—this would allow at most 27 cm of bias on L1 C/A code.)

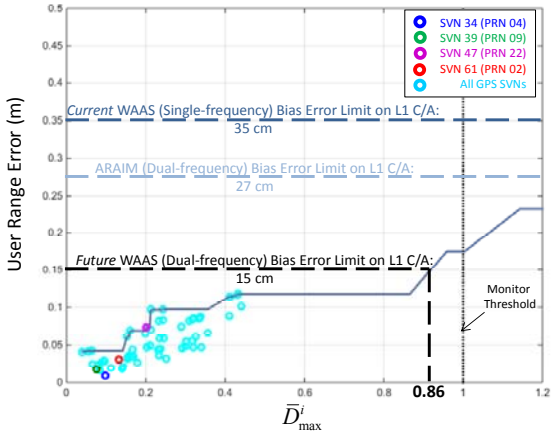

Figure 4. WAAS User Range Error as function of SDM metric $\bar{D}^i_{\max}$. (Dish Data collected on August 1, 2010.)

RESULTS

For all of the SVNs, $\bar{D}^i_{\max}(t)$ was analyzed over a period of approximately 4.5 years—from July 2010 through February 2015. To ensure the threshold was constant and maximum receiver averaging was applied, only data at the minimum detection threshold (i.e., the smallest WAAS UDRE) was used in this analysis.

Figures 5 through 8 plot the average $\bar{D}^i_{\max}(t)$ over one day for each PRN for several years. A single circle is plotted on each of the figures indicating the corresponding WAAS metric value $\bar{D}^i_{\max}$ computed using the dish data as shown in Figure 3. Each plot also shows a series of means taken over 24-hours of data. Above those points, the maximum metric values corresponding to the same 24-hour period are plotted. Note however that since the SVs are only visible to the WAAS network approximately one-half of an actual day and SVs are the maximum observability (i.e., minimum threshold) for a subset of that time (~8 hours), each data point plotted actually corresponds to several days of actual time.

The figures reveal that, with some exceptions, the nominal signal deformations are generally consistent and stable over the total 4.5-year time period. In Figure 5, SVN 34 (PRN 04) provides perhaps the best example of this. The dish data also aligns well with the metric mean

at the beginning of the datasets on both Figures 5 and 6. SVN 39 (PRN 09) also has similarly self-consistent nominal deformation metric data.

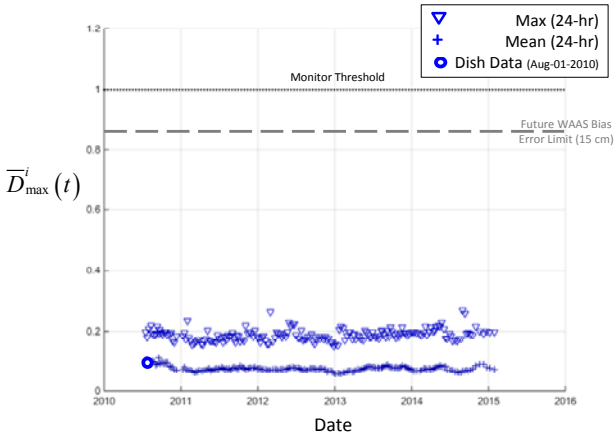

Figure 5. Mean and Max values for WAAS Signal Deformation Monitor metric $\overline{D}^i_{\max}(t)$ for SVN 34 (PRN 04).

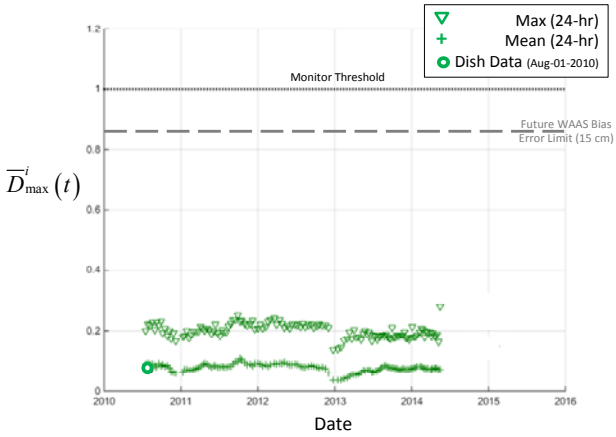

Figure 6. Mean and Max values for WAAS Signal Deformation Monitor metric $\overline{D}^i_{\max}(t)$ for SVN 39 (PRN 09).

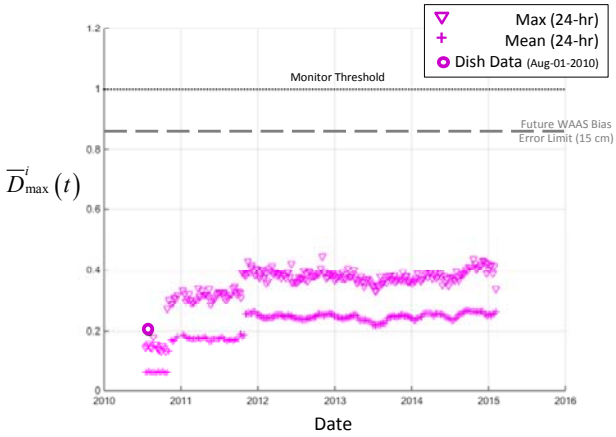

Figure 7. Mean and Max values for WAAS Signal Deformation Monitor metric $\overline{D}^i_{\max}(t)$ for SVN 47 (PRN 22).

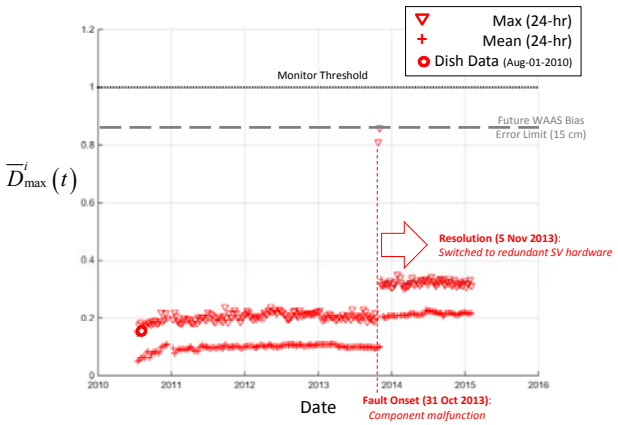

Figure 8. Mean and Max values for WAAS Signal Deformation Monitor metric $\overline{D}^i_{\max}(t)$ for SVN 61 (PRN 02).

Still, two of these four examples contain observable features that are noteworthy. SVN 47 (PRN22) for example, shows several abrupt increases in deformation level. These are not correlated with known anomalies or faults. Some may correspond to planned SV outages; more investigations to this end need to be conducted for verification. Nevertheless, there is no way to know the magnitude (or sign) of the change in the nominal deformation bias error should such a change occur.

In Figure 8, metric data for SVN 61 (PRN 02) reveals two anomalous spikes around late 2013. This was a brief signal anomaly which reportedly lasted from October 31 to November 5 and affected more than just C/A code signal distortion. It was an unpredicted event, and, at epochs not included in these plots, did exceed the monitor trip threshold more than once. However, at the minimum threshold used for the data shown in Figure 8, the maximum value the monitor experienced during this time was approximately 80% of threshold.

It should be noted that for SVNs 47 and 61 (Figures 7 and 8), the dish data more closely corresponds to the 24-hr max, not the mean, of the WAAS metrics plotted at the same time. This is likely due to the fact that there can be a subtle elevation angle-dependence of signal deformations [14]. Recall that the dish data performs a capture at just a single elevation angle. This means the data could represent either a "high" or "low" level of code deformation along the satellite pass.

Figure 9 plots a summary of the max and mean statistics for all the SVs analyzed over the entire 4.5-year time period. The corresponding metrics for the dish data are plotted with the bars for comparison. They are generally bounded by the mean and max values experienced by the WAAS data. (Again, since the dish data only represent a brief (~2-second) snapshot of data, it is likely the WAAS metric captures more of the range of deformations of each SVs as they evolve over all time and elevation angles.)

The largest nominal deformation is likely as large as SVN 40 (PRN 10) and is approximately 55% of the threshold.

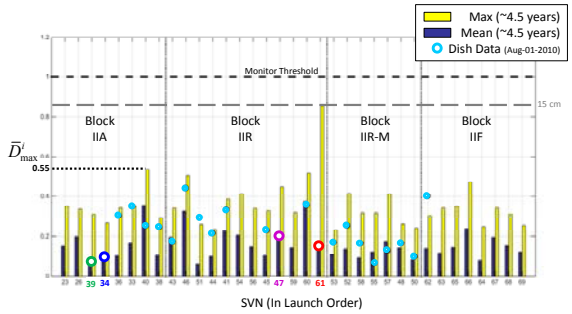

Figure 9. Summary of Mean and Max values for WAAS Signal Deformation Monitor metric $\bar{D}^i_{\max}(t)$ for all SVNs for July 2010 to February 2015.

It follows that a modified assumption on the value of the maximum nominal metric bias has implications for the assumed maximum nominal range bias. Recall that Figure 4 represented the best knowledge of the range bias errors only at the beginning of the data set, when the high-resolution (dish) data was taken. But statistics from the WAAS monitor data suggest the range bias may be somewhat larger. (Refer to Figure 10.) While more dish data is needed to accurately estimate the new biases with established receiver models, this suggests that nominal range biases are closer to the 15 cm error limit for assumed dual-frequency WAAS users than previously assumed.

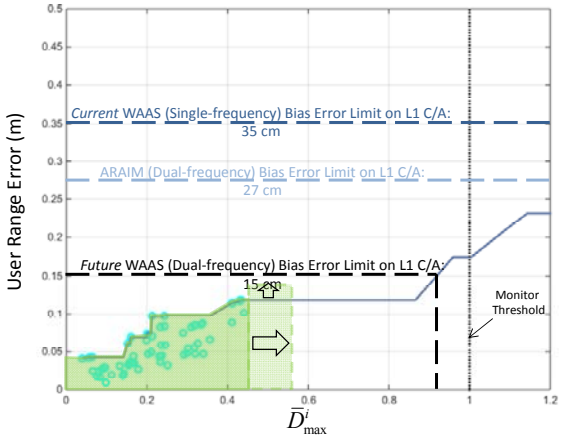

Figure 10. Possible adjustment of maximum nominal WAAS User Range Error based on larger estimated metric $\bar{D}^i_{\max}$.

CONCLUSIONS

More than 4 years of WAAS signal deformation monitoring data for GPS L1 C/A has been collected and analyzed. This monitor is very sensitive to the faults it is designed to detect and, in fact is also quite sensitive to changes in nominal signal deformations. Fortunately, discounting faults and anomalies, the changes have so far been relatively small, and the signals have generally been quite stable. However measurable, unexpected changes due to SV hardware changes can and do occasionally occur.

The high-resolution dish data taken in August of 2010 corresponds reasonably well with the WAAS SDM metric data taken at the same time. It resulted in estimated 12 cm of max nominal bias error at that time, but the WAAS SDM data suggests it could be somewhat larger today.

At present, the most challenging range error limit to validate for high-integrity augmentation systems is the future 15 cm limit for anticipated dual-frequency (L1-L5) WAAS users. These results indicate a need to remain vigilant since the maximum nominal biases are so close to the limit. These nominal deformations should continue to be periodically re-evaluated (e.g., using both dish data and signal deformation monitoring metric data) to ensure the limits are not exceeded.

ACKNOWLEDGMENTS

The authors gratefully acknowledge the FAA for funding the work related to this paper.

APPENDIX

Given elevation angle-dependent *a priori* sigma funcitons ${}_m\sigma^i_j\left(\theta^i_j\right)$, metric weighting factors ${}_m w^i_j$ can be found according to

$$ {}_m w^i_j = \frac{\dfrac{1}{\left[{}_m\sigma^i_j\left(\theta^i_j\right)\right]^2}}{\displaystyle\sum_{j=1}^{J}\left\{\frac{1}{\left[{}_m\sigma^i_j\left(\theta^i_j\right)\right]^2}\right\}} \qquad (11) $$

Then the inter-receiver biases (IRBs) for receiver j (out of a total of J receivers) observing N_j SVs is defined as:

$$ {}^m\hat{b}_j(t) = \frac{1}{N_j}\sum_{i=1}^{N_j} {}^m\hat{b}^i_j(t) \qquad (12) $$

where

$$ {}^m\hat{b}^i_j(t) = \frac{1}{L_b}\,{}^m b^i_j(t) + \frac{L_b - 1}{L_b}\,{}^m\hat{b}^i_j\left(t_{prev}\right) \qquad (13) $$

and

$$ {}^{m}b_j^i(t) = {}^{m}D_j^i(t) - {}^{m}\mathrm{D}^i(t) \quad (14) $$

$$ {}^{m}D^i(t) = \sum_{j=1}^{J}\left[{}_{m}w_j^i(t)\,{}^{m}D_j^i(t)\right] \quad (15) $$

In the above equations, L_b is a long time constant (e.g,. $L_b \geq 500$ seconds).

REFERENCES

[1] Phelts, R. E., Walter, T., Enge, P., "Toward Real-Time SQM for WAAS: Improved Detection Techniques," *Proceedings of the 16th International Technical Meeting of the Satellite Division of the Institute of Navigation*, ION GPS/GNSS-2003, September 2003.

[2] Phelts, R.E., (2001) *Multicorrelator Techniques for Robust Mitigation of Threats to GPS Signal Quality*, Ph.D. Thesis, Stanford University, Stanford, CA.

[3] Hsu, P., Chiu, T., Golubev, Y., Phelts, R. E., "Test Results for the WAAS Signal Quality Monitor," *Proceedings of Position Location and Navigation Symposium*, IEEE/ION PLANS, 2008.

[4] Mitelman, Alexander M., Akos, Dennis M., Pullen, Samuel P., Enge, Per K., "Estimation of ICAO Threat Model Parameters For Operational GPS Satellites,"*Proceedings of the 15th International Technical Meeting of the Satellite Division of The Institute of Navigation (ION GPS 2002)*, Portland, OR, September 2002, pp. 12-19.

[5] Akos, Dennis, Esterhuizen, Stephan, Mitelman, Alexander, Phelts, R. Eric, Enge, Per, "High Gain Antenna Measurements and Signal Characterization of the GPS Satellites," *Proceedings of the 17th International Technical Meeting of the Satellite Division of The Institute of Navigation (ION GNSS 2004)*, Long Beach, CA, September 2004, pp. 1724-1731.

[6] Pini, Marco, Akos, Dennis M., Esterhuizen, Stephan, Mitelman, Alexander, "Analysis of GNSS Signals as Observed via a High Gain Parabolic Antenna," *Proceedings of the 18th International Technical Meeting of the Satellite Division of The Institute of Navigation (ION GNSS 2005)*, Long Beach, CA, September 2005, pp. 1686-1695.

[7] Meurer, M., Thoelert, S., Erker, S., Montenbruck, O., "Potentials for GNSS Signal Enhancements - An Assessment of the Impact of Satellite Imperfections on the Navigation Performance of Todays and Future GNSS," *Proceedings of the 23rd International Technical Meeting of The Satellite Division of the Institute of Navigation (ION GNSS 2010)*, Portland, OR, September 2010, pp. 924-934.

[8] Thoelert, S., Erker, S., Meurer, M., "GNSS Signal Verification with a High Gain Antenna-Calibration Strategies and High Quality Signal Assessment," *Proceedings of the 2009 International Technical Meeting of The Institute of Navigation*, Anaheim, CA, January 2009, pp. 289-300.

[9] Wong, G., Phelts, R.E., Walter, T., Enge, P., "Characterization of Signal Deformations for GPS and WAAS Satellites," *Proceedings of the 23rd International Technical Meeting of The Satellite Division of the Institute of Navigation (ION GNSS 2010)*, Portland, OR, September 2010, pp. 3143-3151.

[10] Wong, G., (2014) *Impact of Nominal Signal Deformations on Satellite Navigation Systems*, Ph.D. Thesis, Stanford University, Stanford, CA.

[11] Minimum Operational Performance Standards (MOPS) for WAAS, DO-229D. *RTCA*.

[12] Phelts, R.E., Blanch, J., Walter, T., Enge, P., "The Effect of Nominal Signal Deformation Biases on ARAIM Users," *Proceedings of the 2014 International Technical Meeting of The Institute of Navigation*, San Diego, California, January 2014, pp. 56-67.

[13] Wong, Gabriel, Chen, Yu-Hsuan, Phelts, R. Eric, Walter, Todd, Enge, Per, "Mitigation of Nominal Signal Deformations on Dual-Frequency WAAS Position Errors,"*Proceedings of the 27th International Technical Meeting of The Satellite Division of the Institute of Navigation (ION GNSS+ 2014)*, Tampa, Florida, September 2014, pp. 3129-3147.

[14] Springer, T., Dilssner, F., "SVN49 and Other Anomalies" *Inside GNSS*, July/Aug. 2009, pp. 33-6.